scientific reports

Check for updates

OPEN

Salmonid sensory system development is affected by climate change driven temperature increases

Aubree E. Jones[1]✉, Matthew J. O'Donnell[2], Amy M. Regish[2] & Jacqueline F. Webb[1]✉

Increases in water temperature due to global climate change are known to alter the course and timing of fish development. The mechanosensory lateral line (LL) system mediates flow-sensing behaviors vital for survival in fishes, but the effects of increased water temperatures resulting from climate change on its development have not been examined. Here LL development was documented in a cold-water salmonid (brook trout, *Salvelinus fontinalis*) reared at the thermograph of a long-term study stream (ambient) and two higher temperatures (+2 and +4 °C) that reflect projected increases within their native range. At these two higher temperatures, fish reach crucial early life history transitions earlier (e.g., hatch, "swim-up" from gravel nests into the water column) and are larger in size through the parr (juvenile) stage. Early forming canal neuromast receptor organs are larger, and the process of canal morphogenesis is also accelerated suggesting potential consequences for neuromast function and presumably for LL-mediated behaviors. A potential mismatch between the timing of transitions in early life history stages, the ability to carry out LL-mediated behaviors (e.g., prey detection), and the timing of the seasonal emergence of their preferred prey, could have serious implications for cold-water salmonid ecology and survival.

Keywords Neuromast, Lateral line, Flow sensing, Ontogeny, Brook trout

As ectotherms, the vast majority of bony fishes are unable to regulate their internal body temperature and are thus affected by increasing water temperatures due to climate change. Effects on certain aspects of morphology, physiology, and behavior have been documented (e.g.,[1–9]), but impacts on the development of the sensory systems that mediate key behaviors that are critical during ontogeny (e.g., prey detection, rheotaxis) have rarely been examined (but refer to[3,8,10]).

The mechanosensory lateral line (LL) system of fishes mediates flow sensing in the context of prey detection, predator avoidance, rheotaxis, navigation, and social communication[11,12]. Neuromast receptor organs, the functional units of the LL system, are comprised of directionally sensitive sensory hair cells that detect unidirectional and oscillatory water flows (0–200 Hz;[12,13]). In a neuromast, all of the ciliary bundles on the surface of the hair cells are embedded in a gelatinous cap, the cupula, which is displaced by water flows, thus stimulating the hair cells. Development of the LL system starts during embryogenesis and continues throughout the early life history of fishes[14,15]. Neuromasts differentiate in embryos and early larvae, then increase in number and size in larvae as two subpopulations of neuromasts become apparent: canal neuromasts and superficial neuromasts. On the head of bony fishes, canal neuromasts become enclosed in canals via a stereotyped process (refer to Fig. 1E–G; defined as Stages 1–4,[16]) that typically starts at the end of the larval period[17,18]. Presumptive canal neuromasts located on the skin (Stage 1) sink into a depression (Stage 2a), walls ossify on either side of the neuromast forming a groove (Stage 2b), and the soft tissue above the neuromast fuses to form a soft canal roof (Stage 3), after which the canal walls fuse within the soft tissue to form an ossified canal segment (Stage 4). Individual canal segments eventually fuse end-to-end to form a continuous canal with periodic pores in the canal roof. In contrast, superficial neuromasts remain on the skin, tend to stay small, and continue to increase in number well beyond the larval stage, in juvenile and adult fishes[18,19].

Canal and superficial neuromasts are also functionally distinct. Canal neuromasts respond to movement of fluid within a canal due to pressure differences between adjacent canal pores and thus act as accelerometers,

[1]Department of Biological Sciences, University of Rhode Island, Kingston, RI 02881, USA. [2]S.O. Conte Research Laboratory, U.S. Geological Survey, Eastern Ecological Science Center, Turners Falls, MA 01376, USA. ✉email: aubree_jones@uri.edu; jacqueline_webb@uri.edu

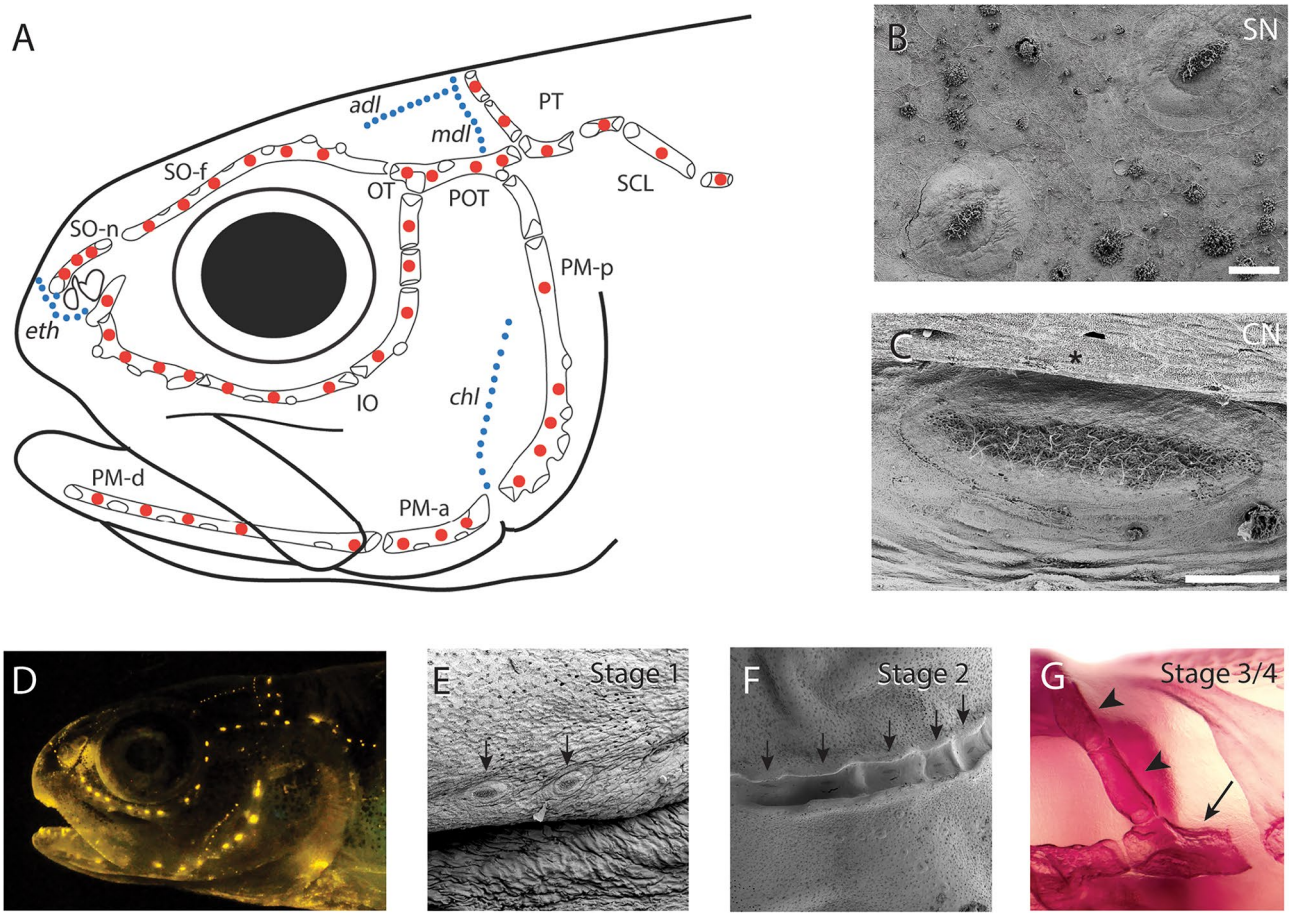

Fig. 1. Representative brook trout cranial lateral line morphology and development. (**A**) Lateral line canals (canal neuromasts = red circles) and lines of superficial neuromasts (blue circles) derived from specimens via vital fluorescent staining and clearing and staining. Canals: SO-n = supraorbital canal, portion associated with the nasal bone, SO-f = supraorbital canal, portion associated with the frontal bone, PT = posttemporal canal, OT = otic canal, POT = post-otic canal, SCL = supracleithral canal, , IO = infraorbital canal, PM-p = preopercular-mandibular canal segments associated with preopercle. The PM-d (canal segments associated with dentary bone) and the PM-a (canal segments associated with anguloarticular bone) comprise the PM-m, the mandibular portion of the preopercular-mandibular canal (analyzed in detail, see text for more details). Superficial neuromast lines: *adl* = antero-dorsal line, *mdl* = midline, *chl* = cheek line, *eth* = ethmoidal line. Adapted from Jones et al.[19]. (**B**,**C**) Scanning electron micrographs (SEM), illustrating (**B**) superficial neuromast (SN) and (**C**) canal neuromast (CN) morphology. (**D**) Fluorescent staining of a 38 mm parr (245 dpf, + 0 °C) with 4-Di-2-ASP in lateral view (images in ventral and dorsal view were also used for counting neuromasts on the left side of the head). (**E**–**G**) Stages of canal morphogenesis. (**E**) SEM of canal neuromasts on skin (Stage 1; arrows = neuromasts), (**F**) in groove with ossified canal walls (Stage 2b; arrows = neuromasts), and in (**G**) cleared and stained specimens showing a canal segment with ossified canal walls and a soft tissue roof (arrow, Stage 3), and two canal segments (arrowheads) with ossified canal walls and roof (Stage 4).

whereas superficial neuromasts respond to the velocity component of flows[11]. Canal neuromasts are especially important for fishes, including salmonids, that live in turbulent or high-flow environments[19–23]. The anatomical and functional transitions that occur with the formation of individual canal segments (e.g., neuromast on the skin, in a groove, enclosed within a canal segment,[24]), the asynchronicity of this process among canal segments, and the overall timing of canal morphogenesis is likely to have consequences for the ontogeny of LL-mediated behaviors[17].

In contrast to other teleosts in which the larval-to-juvenile transformation occurs on the order of a few weeks post-hatch, salmonids have a prolonged larval stage that extends over several months[25]. They lay relatively large demersal eggs and alevin (yolk-sac larvae) "swim up" from their gravel nest into the water column (at ~ 21 mm standard length [SL]), start feeding exogenously (as fry, with the completion of yolk-sac absorption), and then transition to the juvenile (parr) stage ~ 3 to 4 months post-hatch[25]. Increasing water temperatures due to climate change[26,27] have been shown to alter growth rate and timing of these early life history transitions in salmonids in their native ranges[5,6,28].

Brook trout (*Salvelinus fontinalis* Mitchill 1814), a commercially and culturally important cold-water salmonid native to eastern North America[29] can be reared in captivity under controlled conditions, and its growth

rate[30] and metabolic physiology[31] are known to be affected by increased water temperature. Brook trout have a relatively simple LL system (like other salmonids; Fig. 1;[32]) that develops in concert with the slow progression of its early life history[19]. Here we tested the hypothesis that the pattern and timing of LL development in brook trout is altered when reared at higher temperatures that reflect predicted increases within its native range due to current trends in climate change[33]. This is the first study of LL development under climate change scenarios, and it reveals an acceleration of LL development, which may have consequences for the ontogeny of critical LL-mediated behaviors. Furthermore, the acceleration of sensory development, in combination with other environmental threats (e.g., acid rain and freshwater acidification,[34,35],) will likely have compounded effects on the ecology and the potential for survival of this and other salmonid species.

Results and discussion

Brook trout were reared from hatch through the juvenile (parr) stage over ~ 11 months (0 to 327 days post-fertilization, dpf) under three temperature conditions that reflect ambient ("+ 0 °C") and projected (+ 2 °C, + 4 °C) temperatures due to climate change in the long-term study site in western Massachusetts, US from which brood stock were obtained (Fourmile Brook, Northfield, MA;[36];). Projected water temperatures were derived from studies on air temperature increases in the eastern United States[33], which are known to be correlated[36]. The ranges of temperatures used over the course of this study (~ 5 to 18 °C [+ 0 °C, ambient], ~ 7 to 20 °C [+ 2 °C], and ~ 9 to 22 °C [+ 4 °C]; Fig. 2) are commonly used in other studies of brook trout[37].

Fish reared at + 4 °C were larger at hatch and at all life history stages than fish reared at ambient temperature (Fig. 3; ANCOVA with Tukey Contrasts, $p < 0.05$), but fish reared at both + 2 and + 4 °C grew more slowly than fish reared at ambient temperature (Fig. 3; best-fit linear regression, $p < 0.05$, $R^2 = 0.88$ [+ 4 °C], $R^2 = 0.96$ [+ 2 °C], $R^2 = 0.93$ [ambient]). These results are consistent with ecological studies that revealed a correlation between brook trout size and higher stream temperatures in western Massachusetts[29], lab studies that demonstrated the effects of acute exposure to higher temperatures on brook trout growth rate[30], and a study on growth of Atlantic Salmon, *Salmo salar,* reared at higher but constant temperatures[38]. In the current study, the timing of life history transitions was also accelerated at higher temperatures. Hatch (embryo-to-alevin transition; defined as day on

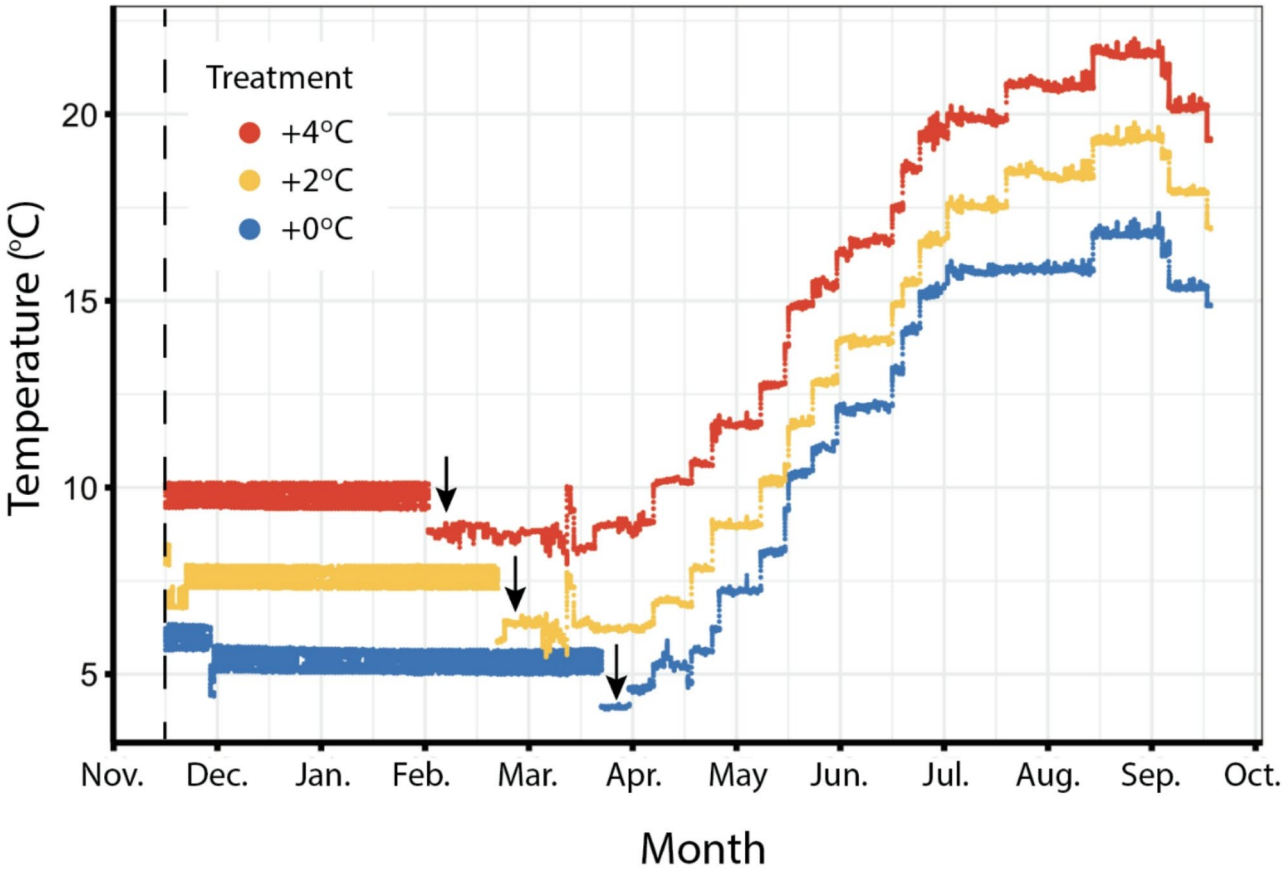

Fig. 2. Temperature regime in rearing system (refer to Materials and Methods section for additional details). Dashed line = fertilization date (November 17, 2020). Thickness of colored bars (Blue, + 0 °C [ambient]; yellow, + 2 °C; red, + 4 °C) reflects diel temperature fluctuations over the winter. Arrows = time at which fish, just prior to swim-up, were moved to 1-m round tanks. Temperature in each of the three treatments (in 1-m round tanks) increased with the same seasonal pattern as in the long-term study stream from which brood stock were obtained (as in[24]).

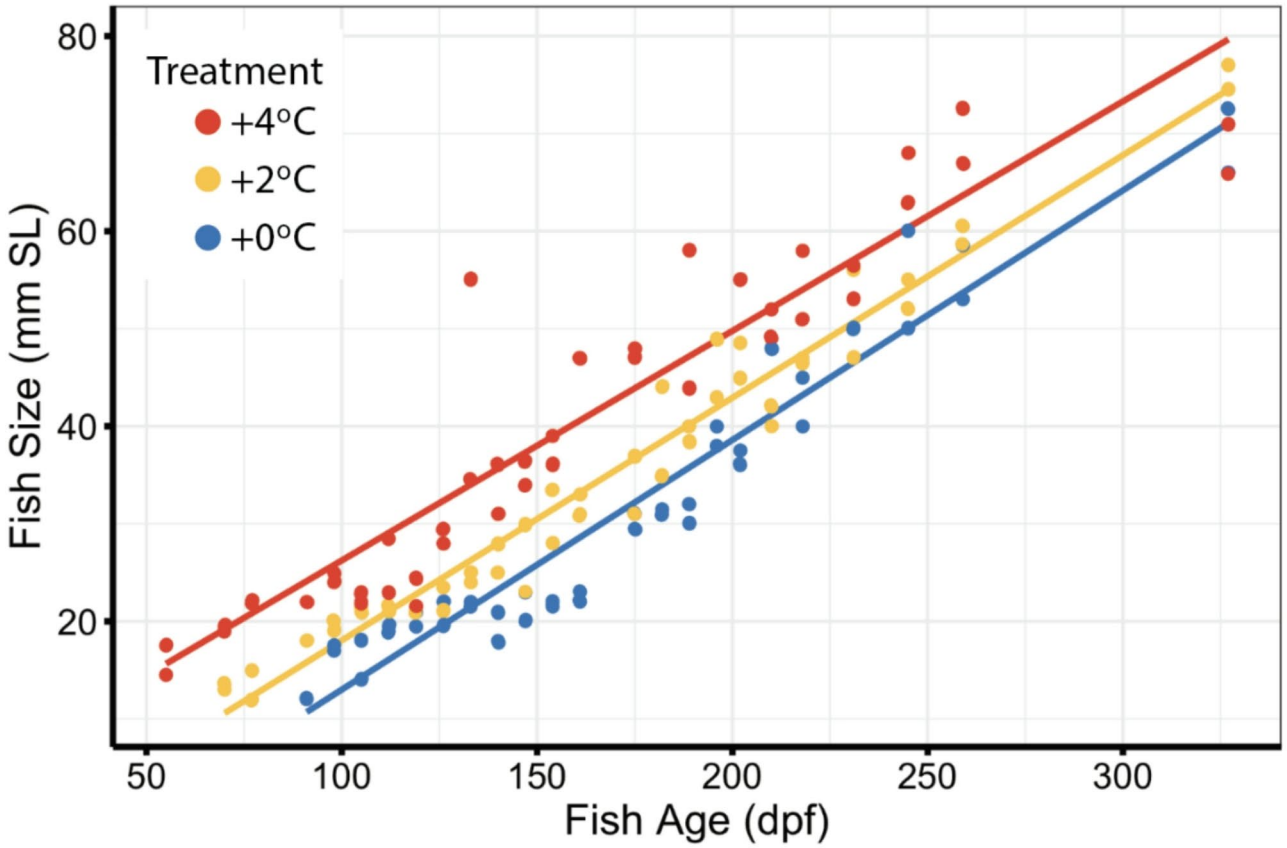

Fig. 3. Size versus age for fish used for vital fluorescent staining in all three temperature treatments (refer to Fig. 1D). Rate of growth (best-fit linear regression, $p < 0.05$): 0.24 mm SL·day^{-1} at + 4 °C (red, $R^2 = 0.88$, n = 44), 0.25 mm SL·day^{-1} at + 2 °C (yellow, $R^2 = 0.96$, n = 47), and 0.26 mm SL·day^{-1} at + 0 °C ([ambient], blue, $R^2 = 0.93$, n = 43). Fish size was significantly larger at + 4 °C than at + 2 °C and + 0 °C (ambient), and fish reared at + 2 °C were significantly larger than those reared at + 0 °C (ambient) (ANCOVA with Tukey Contrasts, $p < 0.05$). SL = standard length, dpf = days post-fertilization.

which 50% of eggs had hatched) tended to occur earlier at + 4 °C (54 dpf) than at + 2 °C (67 dpf) and ambient temperature (92 dpf). Similarly, yolk sac absorption (after the alevin-to-fry transition) tended to occur earlier at + 4 °C (109 dpf) than at + 2 °C (130 dpf) and ambient temperature (181 dpf).

Lateral line (LL) development during the alevin stage was characterized by increases in the number and size of canal and superficial neuromasts (Figs. 4, 5) with observed effects more pronounced at the highest of the three temperatures (+ 4 °C). Canal morphogenesis (enclosure of presumptive canal neuromasts within canals) commenced at the alevin-to-fry transformation (at "swim up") and the rate at which this process continued (Fig. 6) was affected by temperature, but the pattern and relative order of canal morphogenesis (among canals) was not affected.

Neuromast distribution and number is not affected by increased temperature

The distribution of neuromasts on the head (seven series of canal neuromasts and four lines of superficial neuromasts) was revealed by vital fluorescent staining with the mitochondrial dye 4-Di-2-ASP (Fig. 1D, S1). Differences in neuromast number and distribution were not found among the three temperature treatments, suggesting that neuromast patterning[14,15] was not affected by higher temperatures. Soon after hatch (55 dpf [+ 4 °C], 70 dpf [+ 2 °C], 92 dpf [ambient]), neuromasts were present in all seven of the canal series, as well as in three of the four superficial neuromast lines (*eth*, *adl, mdl*); neuromasts in the fourth line (*chl*; Fig. 1A) did not appear until 6–15 days later (by 70 dpf [+ 4 °C], 77 dpf [+ 2 °C], 98 dpf [+ 0 °C, ambient]). Soon after hatch and continuing through the alevin stage, neuromast number increased within each of the seven canal neuromast series and within each of the four superficial neuromast lines (Fig. 4) at all three temperatures. However, the total number of neuromasts did not differ among temperature treatments (ANCOVA, Tukey's Contrasts, n = 43–47 fish/treatment, $p > 0.05$; refer to S2).

At all three temperatures, canal and superficial neuromasts showed contrasting ontogenetic trends (as in other teleosts, 17–18). Prior to the onset of canal morphogenesis (in fish 19–21 mm standard length [SL]; Fig. 4A), canal neuromast number increased but then stabilized soon after the onset of canal morphogenesis, which occurred at similar fish sizes in all three temperature treatments (21.2–23.7 mm SL [+ 4 °C]; 22.0–24.9 mm SL [+ 2 °C]; 21.1–24.4 mm SL [ambient]; 95% confidence intervals, $p < 0.001$ for each temperature,

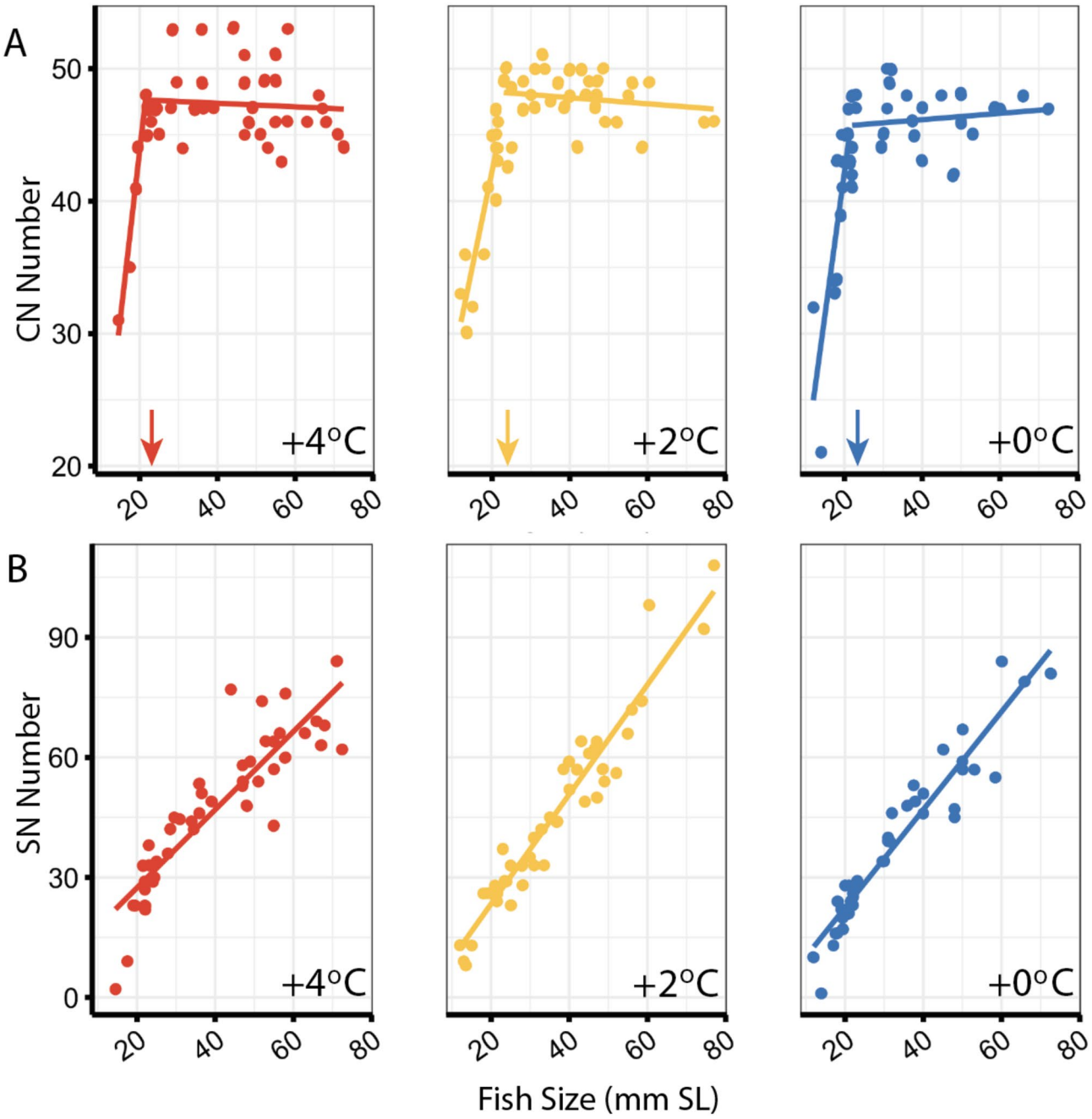

Fig. 4. Ontogenetic increase in canal or superficial neuromast number is not significantly different among temperature treatments (ANCOVA with Tukey Contrasts, $p > 0.05$; data derived from vital fluorescent staining). (**A**) Canal neuromast (CN) number increases linearly with fish size (standard length, mm SL) prior to canal enclosure; a breaking point (arrows, with 95% confidence) occurs at 21.2–23.7 mm SL, 22.0–24.9 mm SL, and 21.1–24.4 mm SL, at + 4 (red), + 2 (yellow), + 0 °C (blue [ambient]), respectively, indicating that number ceases to increase after these points (best-fit linear regression with segmented relationships; see Materials and Methods and S1 for more details). (**B**) Superficial neuromast (SN) number increases linearly with fish size throughout ontogeny (best-fit linear regression parameters reported in text and S1). Note differences in y-axis values for CNs and SNs, indicating that SNs become more numerous than CNs in individuals of comparable sizes.

refer to S3). However, the number of canal neuromasts tended to increase more slowly prior to stabilization in number at + 4 °C (1.94 neuromasts/mm SL; $R^2 = 0.58$, n = 9 fish) and + 2 °C (1.42 neuromasts/mm SL, $R^2 = 0.78$, n = 16 fish) than at ambient temperature (+ 0 °C, 2.19 neuromasts/mm SL, $R^2 = 0.64$, n = 19 fish; best-fit linear regression).

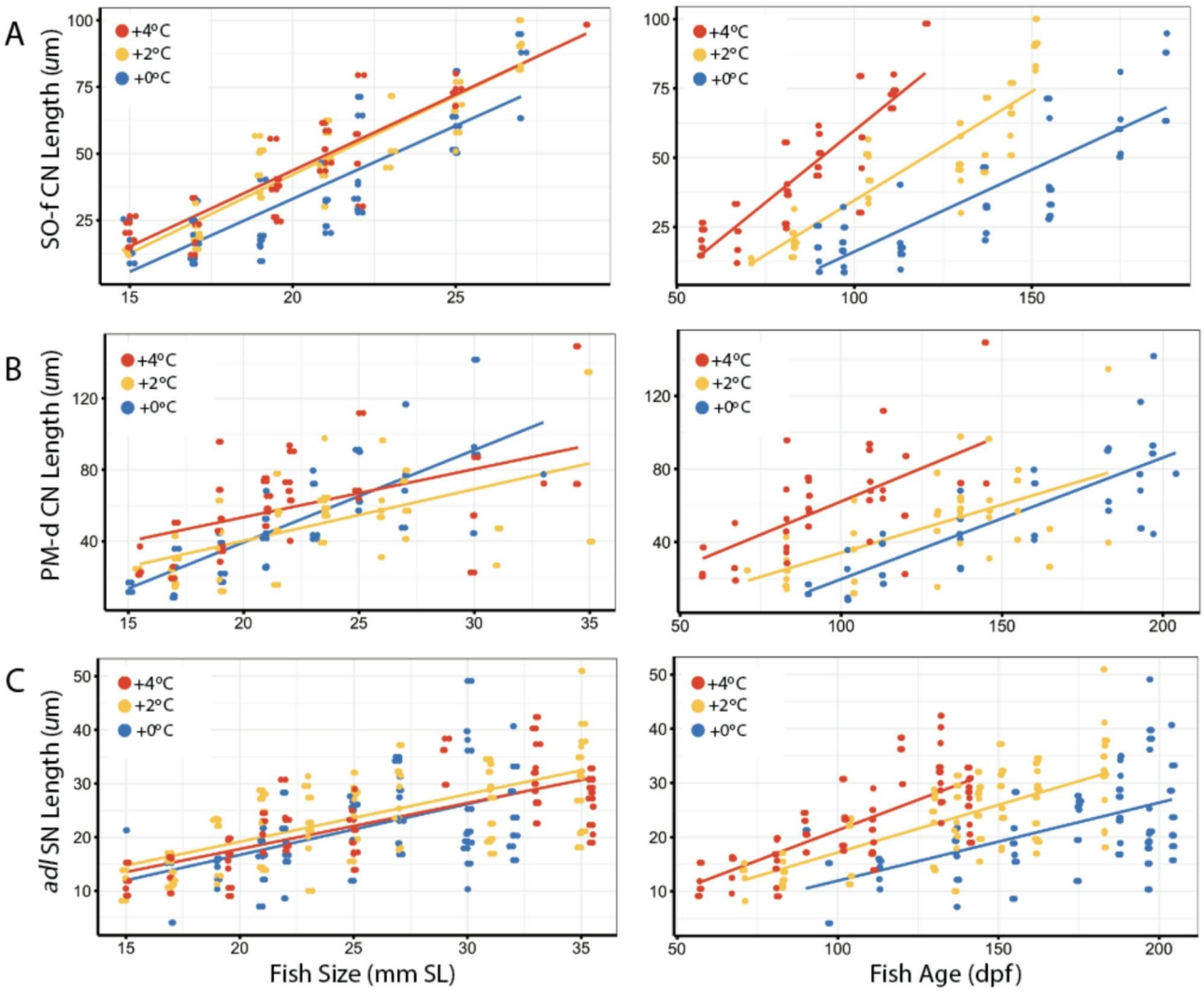

Fig. 5. Size of canal neuromasts (CNs; in SO-f and PM-d canal series) and superficial neuromasts (SNs; in *adl* series) versus fish size (mm standard length [SL], left) and age (days post-fertilization [dpf], right) derived from SEM images. Neuromast size (length) was compared among treatments using ANCOVA with Tukey contrasts, $\alpha = 0.05$; refer to text and S3, S4 for details. (**A**) Size of canal neuromasts in the SO-f canal (n = 70 neuromasts) vs. fish size was significantly larger in fish reared at higher temperatures (red = + 4 °C, $p = 0.002$; yellow = + 2 °C, $p < 0.001$) than at ambient temperature (+ 0 °C [ambient], blue). (**B**) Size of CNs PM-d canal (n = 84 neuromasts) was not significantly different among temperature treatments (ANCOVA, $p > 0.05$, S4). Data presented in A and B include only SO-f and PM-d canal neuromasts prior to their enclosure in canals, after which (in larger/older fishes) they could not be visualized with SEM. (**C**) Size of *adl* SNs (n = 185 neuromasts) was not significantly different among temperature treatments (ANCOVA, $p > 0.05$, S4). SO-f: supraorbital canal segments associated with frontal bone, PM-d: preopercular-mandibular canal segments associated with the dentary bone, *adl* = antero-dorsal SN line; refer to Fig. 1A.

In contrast, superficial neuromast number continued to increase from hatch through the parr stage over a period of several months (Fig. 4B, S3) but the number of superficial neuromasts did not vary among the three temperature treatments (ANCOVA, Tukey's Contrasts, $p > 0.05$, refer to S2). However, superficial neuromast number increased more slowly at + 4 °C (0.97 neuromasts/mm SL; $R^2 = 0.78$, n = 45 fish), than at + 2 °C (1.37 neuromasts/mm SL; $R^2 = 0.93$, n = 47 fish) or at ambient temperature (1.22 neuromasts/mm SL; $R^2 = 0.91$, n = 43 fish). Thus, although the number of canal and superficial neuromasts did not vary among temperatures, the rate of increase in both the number of canal and superficial neuromasts was slightly lower at higher temperatures.

Effects of increased temperature on neuromast size

All neuromasts were oval in shape, but canal neuromasts were more elongate than superficial neuromasts[19]. The sensory hair cells in both types of neuromasts were limited to a central, elongate sensory strip and the axis of best physiological sensitivity (hair cell orientation) was parallel to the long axis (= length) of the neuromast and to the canal series or the line in which the neuromast was found. Scanning electron microscopy (SEM) revealed

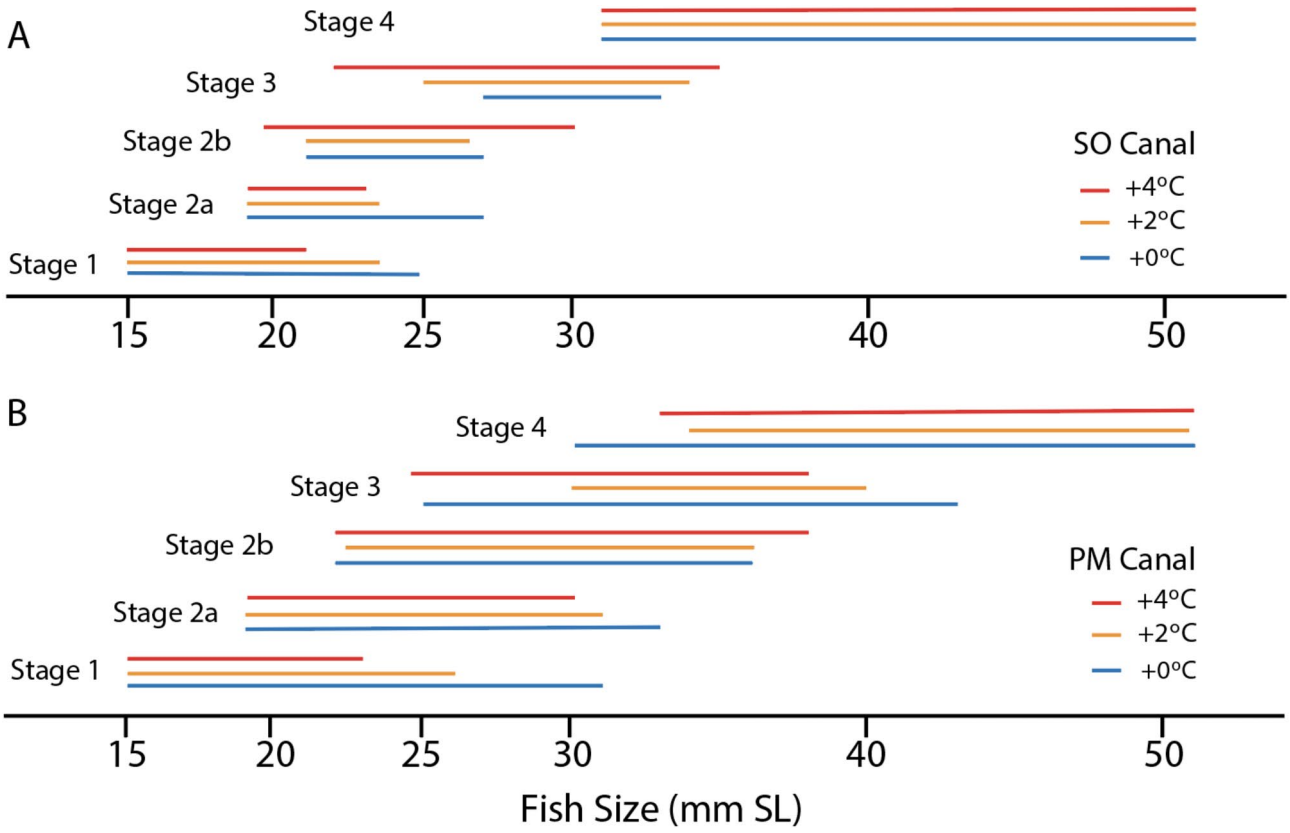

Fig. 6. Onset (first segment at a given stage) and duration of each stage of canal morphogenesis (ending when last segment is observed at a stage) in two cranial lateral line canals for all three temperature treatments (red, + 4 °C; yellow, + 2; blue, + 0 °C [ambient]). (**A**) Supraorbital (SO) canal (associated with the nasal and frontal segments). (**B**) Preopercular-mandibular (PM) canal (associated with the dentary and anguloarticular segments). Onset of canal morphogenesis (Stage 2a) occurs at about the size at which swim up occurs (~ 21 mm SL) in all three temperature treatments. Canal morphogenesis progresses at an accelerated rate at higher temperatures such that more advanced stages of canal morphogenesis are reached in smaller fish at + 4 °C than at + 2 °C or + 0 °C (ambient).

no differences in these features among the three temperature treatments (e.g., Fig. 1B, C). Canal neuromasts increased in size during the alevin and fry stage before their enclosure in canals, after which they could not be visualized with SEM (Fig. 5A, B). Superficial neuromasts continued to increase in size in alevin and well into the parr phase but were consistently smaller than canal neuromasts (Fig. 5C).

Prior to canal enclosure the length of the canal neuromasts varied among temperature treatments in one of the two canal series examined in detail (Fig. 5A, B). Neuromasts in the portion of the supraorbital [SO] canal in association with the frontal bone (SO-f; n = 6–7 neuromasts; 19–27 mm SL), which enclose early, were larger at + 4 °C and + 2 °C than at ambient temperature (ANCOVA, Tukey Contrasts, $p < 0.05$, S4) and increased in size faster at + 4 °C and + 2 °C (5.26 µm/mm SL, $R^2 = 0.80$ and 6.59 µm/mm SL, $R^2 = 0.84$, respectively; best-fit linear regression) than at ambient temperature (3.87 µm/mm SL, $R^2 = 0.75$; Fig. 6; S5). However, neuromasts in the portion of the preopercular-mandibular (PM) canal associated with the dentary bone (PM-d; n = 5–6 neuromasts; 19–33 mm SL), which enclose later than those in the SO-f canal (Fig. 6), did not differ in size among temperature treatments (ANCOVA with Tukey Contrasts, $p > 0.05$; S4). Nevertheless, these canal neuromasts increased in size faster (Fig. 5B, S5) at + 4 °C (6.95 µm/mm SL, $R^2 = 0.30$) than at + 2 °C (5.52 µm/mm SL, $R^2 = 0.31$) and at ambient temperature (6.02 µm/mm SL, $R^2 = 0.59$). Similarly, superficial neuromasts in the *adl* line did not vary in size among temperature treatments (ANCOVA with Tukey Contrasts, $p > 0.05$, Fig. 5C, S4). However, in contrast to both the SO and PM-d canal neuromasts, superficial neuromasts in the *adl* line tended to increase in size more slowly at + 4 °C (0.86 µm/mm SL, $R^2 = 0.86$, n = 56 neuromasts) and + 2 °C (0.89 µm/mm SL, $R^2 = 0.42$, n = 71 neuromasts) than at ambient temperature (0.95 µm/mm SL, $R^2 = 0.23$ n = 58 neuromasts; refer to S5).

In summary, canal neuromasts in the SO canal, but not the PM-d canal, were significantly larger at higher temperatures. In addition, SO canal neuromasts increased in size at a faster rate at higher temperatures, whereas superficial neuromasts in the *adl* line increased in size more slowly. This difference in neuromast growth rate is consistent with the tendency of canal neuromasts to be larger than superficial neuromasts in adult brook trout[19] and in other fishes[16,18]. Interestingly, canal neuromasts were all ~ 95 µm long just prior to enclosure (onset of Stage 3) in all three temperature treatments, which suggests a threshold neuromast size that might be reached

before becoming enclosed in canals. This could be related to tissue-to-tissue signaling during development and/or an adaptive process that would ensure functionality after enclosure within canals, but these hypotheses need to be tested (see[14,15]). The higher rate of increase in the size of canal neuromasts at higher temperatures (+2 °C, +4 °C; Fig. 5) would mean that canal neuromasts reach this size earlier in the growing season. Furthermore, at +4 °C, neuromasts also reach this size in smaller fishes, with the earlier onset of canal morphogenesis in the SO canal.

Canal morphogenesis is accelerated at higher temperatures

The pattern and timing of canal morphogenesis was assessed using SEM (to distinguish among Stages 1, 2a, 2b, and enclosure [Stages 3/4]) and the examination of cleared and stained specimens (required to distinguish among Stages 2b, 3, and 4). The use of these two visualization methods revealed that canal morphogenesis is asynchronous within and among canal series (Fig. 6) at all three temperatures. Canal morphogenesis was not complete (all canal segments at Stage 4) until ~ 8 months post-fertilization (43 mm SL; parr) at ambient temperature but was accelerated at +2 °C and +4 °C so that it was complete in younger fish (i.e., earlier in the growing season; S6, S7).

Morphogenesis of the SO canal commenced (first canal segments at Stage 2a) by the time alevin were 19 mm SL (Fig. 6); thus, given the faster growth rate of fish at higher temperatures, SO canal morphogenesis started earlier in the season at +4 °C (81–83 dpf) and +2 °C (104 dpf) than at ambient temperature (113 dpf). The intermediate stages of canal morphogenesis (Stages 2b, 3) also occurred earlier, and at +4 °C these intermediate stages occurred so much earlier that they were seen in fish at smaller body sizes, despite the faster rate of increase in body size (Fig. 3). At all three temperatures, all SO canal segments were ossified (Stage 4) in fish of approximately the same body size (36–38 mm SL), but this occurred seven weeks earlier at +4 °C (168 dpf) and three weeks earlier at +2 °C (196 dpf) than at ambient temperature (217 dpf).

Morphogenesis of the PM-m canal also started in alevin as small as 19 mm SL, but its development was prolonged so that it was complete ~ 60 days later than the SO canal at ambient temperature, 40 days later than the SO canal at +2 °C, and 10 days later than the SO canal at +4 °C (S6, S7). Again, given the faster growth rate of fish at higher temperatures, the onset of canal morphogenesis occurred in similarly sized fish, but about four weeks earlier at +4 °C (81–83 dpf), and about two weeks earlier at +2 °C (104 dpf) than at ambient temperature (113 dpf). In addition, the intermediate stages of canal morphogenesis (Stages 2b, 3) occurred at approximately the same fish size among temperature treatments but occurred earlier at higher temperatures (+2 °C and +4 °C; Fig. 6B, S7). Completion of PM-m canal morphogenesis (all canal segments at Stage 4) occurred as much as 10.5 weeks earlier at +4 °C (168 dpf, 38 mm SL) and +2 °C (217 dpf, 36 mm SL) than at ambient temperature (242 dpf, 43 mm SL). Thus, canal morphogenesis was complete in fish that were smaller in body size, despite the faster rate of increase in body size at higher temperatures (Fig. 3).

In summary, canal morphogenesis occurred more rapidly at higher temperatures (+2 °C, +4 °C) in both the SO and PM-m canals (Fig. 6) such that the onset (Stage 2a) and completion of canal morphogenesis (Stage 4) occurred in smaller fishes and earlier in the season (in younger fishes). These results are consistent with observations in other species that the timing of LL development is correlated with fish size rather than age[18,39]. However, at the highest temperature (+4 °C), canal development is accelerated (e.g., with respect to fish age and the intermediate stages of canal morphogenesis also occur at a smaller fish body size at +4 °C than at +2 °C and + 0 °C, ambient temperature). Thus, a consistent pattern emerges, where the increase in neuromast size and progression of canal morphogenesis are accelerated relative to both fish size and age in the highest of the three temperature treatments.

The effect of increased rearing temperature on the rate of canal morphogenesis was different between the SO (one of the first canals to complete morphogenesis) and the PM-m (one of the last canals to complete morphogenesis)[19]. This suggests that canal morphogenesis, and perhaps other developmental processes that occur early and rapidly during ontogeny are more likely to be affected by increased temperatures than processes that occur later and/or more slowly during ontogeny.

The accelerated rate of LL canal development at higher temperatures is consistent with effects of increased temperature on the development of other metabolically expensive calcified structures (otoliths, vertebral bone, scales;[2,3,8,9]). Calcium recruitment for developmental processes could present a challenge under climate change conditions as rising CO_2 levels can lead to acidification of freshwater environments (reviewed in[34]). Streams in New England watersheds are already acidified as a result of acid rain and precipitation events that have reduced buffering capacity[35]. Decreased calcium availability in acidified watersheds[34] has known physiological effects in migratory salmonids in this region[40,41] and in European freshwater systems[42]. The complexities of calcium dynamics in freshwater habitats, including the effects of temperature dependent solubility, geological processes (e.g., allochthonous input), CO_2 levels, and seasonal variation in availability of dietary calcium, raise questions about whether fish would be able to obtain sufficient calcium for the demands of accelerated canal morphogenesis and higher overall growth rates (Fig. 3) at higher temperatures (Fig. 6, S6, S7). Aquaculture practices, like those used in this study, may provide adequate dietary calcium[43] under experimental conditions but it is unclear whether sufficient dietary calcium would be available to carry out fundamental metabolic and developmental processes in natural habitats under climate change conditions.

Behavioral and ecological implications of accelerated lateral line development

The effects of higher water temperatures on the development of the LL system are predicted to have functional and ecological consequences for brook trout and likely for other salmonids. This study showed that the number and distribution (patterning) of canal and superficial neuromasts, the overall pattern of canal morphogenesis, and the presence of asynchronicity in the development of canal segments within and among canals were not affected by higher rearing temperature. The genetic and developmental factors regulating neuromast patterning

have been studied in detail in zebrafish, *Danio rerio*[17], but the factors controlling the order and rate of canal morphogenesis are not known. In the current study, neuromast patterning would occur during the winter in embryos and early alevin (Fig. 2). The tendency for overwintering temperature to be consistent in nature[26] may explain the lack of variation in neuromast patterning among temperature treatments. Alternatively, this may be explained by the high thermal tolerance during the embryonic period of fishes (reviewed in[1]).

In contrast, aspects of the development of the LL system that occur later, during the spring, were affected by increased rearing temperatures during the study period. The rate at which temperatures increased was similar among treatments (Fig. 2), so absolute temperature may explain the observed acceleration in canal morphogenesis at + 2 °C and + 4 °C treatments compared to the ambient temperature treatment. While the mechanisms of these developmental processes are not known, the acceleration of canal morphogenesis means that not only is canal morphogenesis completed in a shorter period of time, but that the duration of the intermediate developmental stages (Stages 1–4), through which each canal segment progresses, is shortened. This affects the time interval during which the neuromast within a canal segment has particular functional properties (e.g., on skin, in groove, enclosed in soft tissue or in ossified canal; segments;[13,24]). Thus, such changes to developmental timing are likely to affect LL-mediated behaviors in fry and parr.

Higher temperatures also affect the physiology and biomechanics of individual neuromasts. Temperature is known to affect neuromast sensitivity[44], which may further compound changes in canal neuromast morphology as documented in this study (Fig. 5, S4, S5). Larger neuromasts tend to have more hair cells[16], which would likely increase the flexural stiffness of the cupula making the neuromasts less sensitive to flows (as in larval zebrafish, *Danio rerio*;[45]). At higher temperatures, the higher growth rate of canal neuromasts suggests higher rates of hair cell differentiation (as in the amphibian ear,[46,47]). Hair cells are constantly active (with a resting firing rate) and are thus energetically expensive[46,48], so larger neuromasts with more hair cells likely have higher energetic costs. Thus, higher temperatures may alter neuromast function with consequences for LL-mediated behaviors.

The observed changes in developmental processes and LL morphology can further be considered in an ecological context with respect to their early life history transitions. In brook trout reared at higher temperatures (+ 2 and + 4 °C), yolk sac absorption occurs ~ 3 to 7 weeks earlier and fish begin exogenous feeding during the alevin to fry transition 4–8 weeks earlier in the season than those reared at ambient temperature. Thus, more developmentally advanced fishes are found in the water column earlier in the season at higher temperatures. Nevertheless, the onset of canal morphogenesis is still synchronized with a key developmental transition, occurring just before "swim up" (at ~ 19 mm SL) when alevin (yolk-sac larvae) leave their gravel nests and enter the water column (at ~ 21 mm SL) and transition to the fry stage (at ~ 23 mm SL; Fig. 2).

The timing of the onset of critical behaviors of fishes in the water column also becomes important. The LL system is known to function in predator avoidance, prey detection, and rheotaxis in young fishes[49,50]. After swim-up, predator avoidance will certainly be crucial for survival of brook trout fry and parr, and temperature effects on neuromast function could affect such behaviors. Avoidance behavior in adult salmonids is known to be affected by rearing conditions (aquaculture vs. wild-reared[51];), so the effect of increased temperatures on this behavior could be examined. A mismatch in the timing of the onset of exogenous feeding and the emergence of preferred prey species[52] may present a critical challenge for these fishes, although there is some evidence that emergence of aquatic insect larvae, the preferred prey of post-swim-up brook trout, occurs earlier in the season at higher water temperatures[53]. Regardless of prey emergence patterns, foraging strategies are likely to be affected at higher temperatures. If daytime stream temperatures exceed the thermal tolerance for brook trout[25,29], they may be forced to seek thermal refuges[54] or to forage nocturnally (as reported in salmonids, including adult brook trout[21,23,55] and fry[48,56,57]). Adult salmonids entrain behind objects during diurnal and nocturnal foraging behavior via LL-mediated rheotaxis[21–23], and post-swim-up brook trout that feed nocturnally are likely to rely on LL input as well. Such behavioral complications are in addition to and are consequences of the changes to neuromast function due to altered morphology (increased neuromast size and changes to sensitivity) and developmental timing. Thus, under climate change scenarios, morphological and functional alterations to neuromasts may present challenges for prey detection behavior, particularly during the critical period immediately following swim-up.

Finally, increased fish size and acceleration of transitions between life history stages, increases in rates of neuromast growth (Fig. 3), and the timing of canal morphogenesis (Fig. 6) at higher temperatures were more dramatic in fish reared at + 4 °C than at + 2 °C. This suggests that the effects of increased temperature on LL development—and potentially developmental processes more broadly—are graded with the degree of the changes in water temperature. This study has revealed effects of increased temperature on major ontogenetic processes (life history transitions) and on the development of an important sensory system as a result of just a 2–4 °C degree increase in water temperature. Thus, it is predicted that the observed acceleration in development due to increased rearing temperature, which reflect conditions under climate change, resulted in the morphological differences observed in this study (but refer to[58–61]). It is predicted that they will impact LL-mediated behaviors critical for the early life history stages of brook trout and thus for the ecology and potentially survival of this species and of salmonids more broadly.

Materials and methods

Rearing of fish

All methods reported are in accordance with ARRIVE guidelines (Animal Research: Reporting of In Vivo Experiments). Wild brook trout were collected from Fourmile Brook, Northfield, MA (October 2015) and maintained at the U.S. Geological Survey (USGS) Eastern Ecological Science Center (EESC), S.O. Conte Research Laboratory (Turners Falls, MA) under conditions reflecting thermal conditions of a nearby, long-term study stream ("ambient temperature";[26]). On November 19, 2020, trout were strip spawned and four families were created: Family 1) three females and two males (4382 eggs), Family 2) three females and two males (4946

eggs), Family 3) two females and two males (2920 eggs), and Family 4) three females and two males (4853 eggs). After fertilization and water hardening, the number of viable eggs per family was estimated by counting the number of eggs per mL, and then extrapolated to the total volume of eggs for that family. In total, each treatment received approximately 5700 fertilized eggs. After fertilization, eggs were divided and placed into three egg banks (insulated vertical stack incubators) with partially recirculated (~ 1 L min^{-1} 'new' water introduced to each egg bank), dechlorinated municipal water, UV treated and chilled to temperatures relevant to their treatment, under a 24-h dark cycle (mimicking conditions within redds). Prior to swim-up (and thus prior to completion of yolk-sac absorption, and onset of exogenous feeding) alevin were moved to three, round flow-through rearing tanks (~ 1 m wide × 0.6 m deep).

The rearing tanks were initially supplied with tempered well water at three different overwintering temperatures: (1) ambient temperature ("+ 0 °C"; based on the thermal regime of the long-term study stream;[26]), (2) ambient temperature plus 2 °C ("+ 2 °C"), and (3) ambient temperature plus 4 °C ("+ 4 °C"). These temperature treatments are similar to those used in other studies of brook trout thermal stress and are in the stressful, but not lethal, range for brook trout[30,31]. The experimental thermal regime (Fig. 2) used in this study mirrored typical seasonal changes in water temperature in a stream in the native range of brook trout[26,37]. However, the overwintering temperature in the experimental husbandry system (~ 5 °C; in Nov.–Feb.) did not reach the lowest levels that may occur in nature[33] and that are still likely to be reached under climate change conditions (close to 0 °C).

After moving fish to the round tanks, the water temperature in each tank was gradually increased in a typical seasonal pattern (Fig. 2, as in[26]) with maximum temperatures of ~ 18, 20, and 22 °C in the + 0 (ambient), + 2, and + 4 °C treatments, respectively (Fig. 2). Alevin and fry were fed twice daily, and then as fish size increased and feeding appeared volitional, food size was increased (BioVita Starter, then BioTrout; Bio-Oregon, Westbrook, ME) and fish were fed once per day. After approximately one month after being moved to the round tanks, fish were split into two round tanks per treatment. Similar fish densities (hundreds of fish) and food rations were maintained in the stock tanks for each temperature treatment, so observed size differences across tanks (among temperature treatments) were likely to be the result of water temperature differences and not fish density or feeding regime. Additionally, the trout used in this study are F_1 of wild-caught fishes, and thus were not likely affected by captive rearing conditions (refer to[51,62]).

Sampling commenced in January 2021 on "day-of-hatch" (the day on which ~ 50% of the eggs had hatched; visually assessed). This occurred at 91-dpf, 67-dpf, and 54-dpf, at + 0 °C (ambient temperature), + 2 °C, and + 4 °C, respectively. Two to three fish were sampled from each temperature treatment twice a week (from hatch to well into the parr stage), anesthetized in 0.1 M MS-222, and fixed in 4% paraformaldehyde (PFA; ACROS #41678-001) in 100 mmol L^{-1} phosphate-buffered saline (= 4% buffered PFA) or in 10% buffered formalin (Fisher Scientific, #427-098). Flexion is complete in brook trout prior to day-of-hatch, so anaesthetized fish were all measured to the nearest 0.5 mm as standard length (SL) during preparation for vital staining or after fixation. Rearing of fish was carried out under USGS EESC approved IACUC protocol #2021-07C, and all experiments were carried out in accordance with the relevant guidelines and regulations.

Vital fluorescent staining

Vital staining of neuromasts using 4-Di-2-ASP, a fluorescent mitochondrial stain (Sigma #D34138), was conducted at the S.O. Conte Research Laboratory (Jan.–Oct. 2021) following a University of Rhode Island approved IACUC protocol (#AN1718-016). Fish reared at + 0 °C (ambient), + 2 °C, and + 4 °C were sampled weekly starting on day-of-hatch or soon thereafter (at 55, 70, or 91 dpf to 218 dpf; for + 0 °C (ambient), + 2 °C, + 4 °C treatments, respectively), then biweekly (231–259 dpf), and at 327 dpf after canal morphogenesis was complete (n = 44–47 fish/treatment; 14.5–77 mm SL, alevin, fry and parr). Individual fish were allowed to swim in a 0.0024% solution of 4-Di-2-ASP (in rearing system water) for 5–10 min, rinsed in rearing system water for 5 min., and anaesthetized in 0.02% MS-222 (Sigma A-5040; buffered to 8.4 pH with sodium bicarbonate) in system water until posture could not be maintained and opercular movement ceased. Neuromasts were visualized using a fluorescence viewing system (NIGHTSEA, Electron Microscopy Services, #SFA-RB, Lexington, MA) and stereoscope (Wild Heerbrugg M5A, Heerbrugg, Switzerland) equipped with a digital camera (Nikon D500 DSLR) and 0.25X projection lens. Images were acquired (iDigiCam, v. 2.1.6 or Adobe Lightroom Classic, v. 12.5.1), after which fish were euthanized in 0.04% buffered MS-222, and fixed in 4% paraformaldehyde in 10 mM L^{-1} phosphate-buffered saline (4% PFA). Images taken in multiple views (e.g., Fig. 1D, S1) were used to determine neuromast number and distribution on one side of the head (right side, unless noted). Image stacks were constructed using the auto-blend layers tool (Adobe Photoshop, v. 25.3.1) and neuromast distribution maps were generated using Adobe Illustrator (v. 28.4.1).

All statistical analyses were carried out using RStudio (v. 1.4.1717;[63]). Linear regressions with segmented relationships (R package segmented,[64]) were used to model canal neuromast number versus fish size (mm SL) and linear regressions were used to model the relationship of number of superficial neuromasts to fish size for all three temperature treatments (S1). Total numbers of canal and superficial neuromasts were not normally distributed (Shapiro–Wilk Test, $p < 0.05$). However, the relationship between neuromast number and fish size was linear ($p < 0.05$) and the variances among the three treatments were not significantly different (Levene's Test, $p > 0.05$), so neuromast numbers were compared among the three temperature treatments using ANCOVA with Tukey Contrasts (residuals normally distributed, Shapiro–Wilk Test $p = 0.23$). Significance was defined using $\alpha = 0.05$ for all analyses.

Scanning electron microscopy (SEM) and clearing and staining for bone

Fish from the ontogenetic series that had been fixed in 4% PFA (57–145 dpf, 15–35.5 mm SL [+ 4 °C]; 71–183 dpf, 15–35 mm SL [+ 2 °C]; 90–287 dpf, 15–33 mm SL [+ 0 °C, ambient]; n = 18 fish/treatment) were dehydrated

in a graded ethanol series, critical point dried out of liquid CO_2 (Leica MED 020), mounted on aluminum stubs with adhesive carbon disks (Ted Pella, Inc., 16084-2, 16327) and sputter coated with 15 nm platinum. Digital images were acquired on a Zeiss Supra 40VP SEM (at 3 kV and ~ 10 µm working distance) (Jena, Germany) at the Marine Biological Laboratory (Woods Hole, MA). The size of canal neuromasts in the supraorbital (SO) canal series associated with the frontal bone (SO-f; in fish 19–27 mm SL, n = 70 neuromasts), the size of canal neuromasts in the preopercular mandibular (PM) canal series associated with the dentary bone (PM-d; in fish 19–33 mm SL, n = 84 neuromasts), and the size of superficial neuromasts in the antero-dorsal line (*adl*; representative of the four superficial neuromast lines; in 15–35 mm SL fish, n = 185 neuromasts; Fig. 1A;[19]) were measured in SEM images (left side of the head unless otherwise noted, ImageJ, v. 2.3). Canal and superficial neuromasts were also measured in the largest individual from each of the three temperature treatments prior to their enclosure in canals (SO-f, 27 mm SL; PM-d, 33 mm SL). Canal and superficial neuromast length were normally distributed (Shapiro–Wilk Test, $p > 0.05$), modeled using linear regression, and compared among temperature treatments using ANCOVA with Tukey Contrasts (residuals were normally distributed, Shapiro–Wilk Tests: $p = 0.17$ [SO]; $p = 0.53$ [PM-d]; $p = 0.20$ [*adl*]).

Additional fish from the same ontogenetic series as described above (97–301 dpf (+ 4 °C], 21–68 mm SL; 134–383 dpf [+ 2 °C], 21–70 mm SL; 146–383 dpf [ambient], 21–69 mm SL; 12–13 fish/treatment) were fixed in 4% PFA and enzymatically cleared and stained (for ossified bone only;[65]) to document the pattern and timing of development of individual canal segments in the SO and PM-m canals (scored as Stages 1–4; defined in[16]).

Data availability

Data and code are available on GitHub (https://github.com/aubreejones/brooktroutdevo_temp). Image data are being used for ongoing projects, and thus are not yet public, but samples of image data are available in a public data repository (https://zmaportal.org/zmaportal/larequest.php?request=studyOverview_public&StudyID=38&instit=ZMA_ZMA).

Received: 4 December 2024; Accepted: 22 April 2025
Published online: 01 July 2025

References

1. Pottier, P. et al. Developmental plasticity in thermal tolerance: Ontogenetic variation, persistence, and future directions. *Ecol. Lett.* **25**(10), 2245–2268. https://doi.org/10.1111/ele.14083 (2022).
2. Gauldie, R. W., Coote, G., West, I. F. & Radtke, R. L. The influence of temperature on the fluorine and calcium composition of fish scales. *Tissue Cell* **22**(5), 645–654. https://doi.org/10.1016/0040-8166(90)90061-D (1990).
3. Townsend, D. W., Radtke, R. L., Corwin, S. & Libby, D. A. Strontium: calcium ratios in juvenile Atlantic herring *Clupea harengus* L. otoliths as a function of water temperature. *J. Exp. Mar. Biol. Ecol.* **160**(1), 131–140. https://doi.org/10.1016/0022-0981(92)90115-Q (1992).
4. Farrell, A. P. Environment, antecedents and climate change: Lessons from the study of temperature physiology and river migration of salmonids. *J. Exp. Biol.* **212**(23), 3771–3780. https://doi.org/10.1242/jeb.023671 (2009).
5. Wedekind, C. & Kueng, C. Shift of spawning season and effects of climate warming on developmental stages of a grayling (Salmonidae). *Conserv. Biol.* **24**(5), 1418–1423. https://doi.org/10.1111/j.1523-1739.2010.01534.x (2010).
6. Pankhurst, N. W. & Munday, P. L. Effects of climate change on fish reproduction and early life history stages. *Mar. Freshw. Res.* **62**(9), 1015–1026. https://doi.org/10.1071/MF10269 (2011).
7. Little, A. G., Loughland, I. & Seebacher, F. What do warming waters mean for fish physiology and fisheries?. *J. Fish Biol.* **97**(2), 328–340. https://doi.org/10.1111/jfb.14402 (2020).
8. Loeppky, A. R. et al. Influence of ontogenetic development, temperature, and pCO2 on otolith calcium carbonate polymorph composition in sturgeons. *Sci. Rep.* **11**(1), 1–10. https://doi.org/10.1038/s41598-021-93197-6 (2021).
9. Ytteborg, E., Baeverfjord, G., Torgersen, J., Hjelde, K. & Takle, H. Molecular pathology of vertebral deformities in hyperthermic Atlantic salmon (*Salmo salar*). *BMC Physiol.* **10**, 1–16. https://doi.org/10.1186/1472-6793-10-12 (2010).
10. Kelley, J. L., Chapuis, L., Davies, W. I. & Collin, S. P. Sensory system responses to human-induced environmental change. *Front. Ecol. Evol.* **6**, 95. https://doi.org/10.3389/fevo.2018.00095 (2018).
11. van Netten, S. M. V. & McHenry, M. J. The biophysics of the fish lateral line. In *The Lateral Line System* (eds Coombs, S. et al.) 99–119 (Springer, 2013). https://doi.org/10.1007/978-1-4614-8851-4.
12. Mogdans, J. Sensory ecology of the fish lateral-line system: Morphological and physiological adaptations for the perception of hydrodynamic stimuli. *J. Fish Biol.* **95**(1), 53–72. https://doi.org/10.1111/jfb.13966 (2019).
13. McHenry, M. J. & Liao, J. C. The hydrodynamics of flow stimuli. In *The Lateral Line System* (eds Coombs, S. et al.) 73–98 (Springer, 2013). https://doi.org/10.1007/978-1-4614-8851-4.
14. Ghysen, A., Dambly-Chaudière, C., Coves, D., de La Gandara, F. & Ortega, A. Developmental origin of a major difference in sensory patterning between zebrafish and bluefin tuna. *Evol. Dev.* **14**(2), 204–211. https://doi.org/10.1111/j.1525-142X.2012.00529.x (2012).
15. Iwasaki, M., Yokoi, H., Suzuki, T., Kawakami, K. & Wada, H. Development of the anterior lateral line system through local tissue-tissue interactions in the zebrafish head. *Dev. Dyn.* **249**(12), 1440–1454. https://doi.org/10.1002/dvdy.225 (2020).
16. Webb, J. F. & Shirey, J. E. Postembryonic development of the cranial lateral line canals and neuromasts in zebrafish. *Dev. Dyn.* **228**(3), 370–385. https://doi.org/10.1002/dvdy.10385 (2003).
17. Webb, J. F. Morphological diversity, development, and evolution of the mechanosensory lateral line system. In *The Lateral Line System* (eds Coombs, S. et al.) 17–72 (Springer, 2014). https://doi.org/10.1007/978-1-4614-8851-4.
18. Becker, E. A., Bird, N. C. & Webb, J. F. Post-embryonic development of canal and superficial neuromasts and the generation of two cranial lateral line phenotypes. *J. Morphol.* **277**(10), 1273–1291. https://doi.org/10.1002/jmor.20574 (2016).
19. Jones, A. E., Rizzato, P. P. & Webb, J. F. Development of the cranial lateral line system of Brook Trout, *Salvelinus fontinalis* (Teleostei: Salmonidae): Evolutionary and ecological implications. *J. Morphol.* **285**(8), e21754. https://doi.org/10.1002/jmor.21754 (2024).
20. Engelmann, J., Hanke, W. & Bleckmann, H. Lateral line reception in still-and running water. *J. Comp. Physiol. A.* **188**(7), 513–526. https://doi.org/10.1007/s00359-002-0326-6 (2002).
21. Coombs, S., Bak-Coleman, J. & Montgomery, J. Rheotaxis revisited: A multi-behavioral and multisensory perspective on how fish orient to flow. *J. Exp. Biol.* **223**(23), jeb223008. https://doi.org/10.1242/jeb.223008 (2020).
22. Montgomery, J. C., Baker, C. F. & Carton, A. G. The lateral line can mediate rheotaxis in fish. *Nature* **389**(6654), 960–963. https://doi.org/10.1038/40135 (1997).

23. Liao, J. C. The role of the lateral line and vision on body kinematics and hydrodynamic preference of rainbow trout in turbulent flow. *J. Exp. Biol.* **209**(20), 4077–4090. https://doi.org/10.1242/jeb.02487 (2006).
24. Schwarz, J. S., Reichenbach, T. & Hudspeth, A. J. A hydrodynamic sensory antenna used by killifish for nocturnal hunting. *J. Exp. Biol.* **214**(11), 1857–1866. https://doi.org/10.1242/jeb.051714 (2011).
25. Birnie-Gauvin, K., Thorstad, E. B. & Aarestrup, K. Overlooked aspects of the *Salmo salar* and *Salmo trutta* life cycles. *Rev. Fish Biol. Fisheries* **29**(4), 749–766. https://doi.org/10.1007/s11160-019-09575-x (2019).
26. Letcher, B. H. et al. A hierarchical model of daily stream temperature using air-water temperature synchronization, autocorrelation, and time lags. *PeerJ* **4**, e1727. https://doi.org/10.7717/peerj.1727 (2016).
27. Merriam, E. R., Fernandez, R., Petty, J. T. & Zegre, N. Can brook trout survive climate change in large rivers? If it rains. *Sci. Total Environ.* **607**, 1225–1236. https://doi.org/10.1016/j.scitotenv.2017.07.049 (2017).
28. Carter, K. The effects of dissolved oxygen on steelhead trout, coho salmon, and chinook salmon biology and function by life stage. California Regional Water Quality Control Board, North Coast Region, 10 (2005).
29. Meisner, J. D. Effect of climatic warming on the southern margins of the native range of brook trout, *Salvelinus fontinalis*. *Can. J. Fish. Aquat. Sci.* **47**(6), 1065–1070. https://doi.org/10.1139/f90-122 (1990).
30. McCormick, J. H., Hokanson, K. E. & Jones, B. R. Effects of temperature on growth and survival of young brook trout, *Salvelinus fontinalis*. *J. Fish. Board Can.* **29**(8), 1107–1112. https://doi.org/10.1139/f72-165 (1972).
31. Chadwick, J. G. & McCormick, S. D. Upper thermal limits of growth in brook trout and their relationship to stress physiology. *J. Exp. Biol.* **220**(21), 3976–3987. https://doi.org/10.1242/jeb.161224 (2017).
32. Nakae, M. & Hasegawa, K. The lateral line system and its innervation in the masu salmon *Oncorhynchus masou masou* (Salmonidae). *Ichthyol. Res.* https://doi.org/10.1007/s10228-021-00843-0 (2021).
33. Christensen, J.H., Hewitson, B., Busuioc, A., Chen, A., Gao, X., Held, I., Jones, R., Kolli, R.K., Kwon, W., Laprise, R., Magaña Rueda, V., Mearns, L., Menéndez, C.G., Räisänen, J., Rinke, A., Sarr, A. & Whetton, P. Regional climate projections. In *Climate Change 2007: The Physical Science Basis. Contribution of Working Group I to the Fourth Assessment Report of the Intergovernmental Panel on Climate Change* (eds. S. Solomon, D. Qin, M. Manning, Z. Chen, M. Marquis, K.B. Averyt, M. Tignor. and H.L Miller). (Cambridge University Press, 2007). https://doi.org/10.1007/978-81-322-1967-5_4
34. Hasler, C. T., Butman, D., Jeffrey, J. D. & Suski, C. D. Freshwater biota and rising pCO_2?. *Ecol. Lett.* **19**, 98–108. https://doi.org/10.1111/ele.12549 (2016).
35. Driscoll, C.T. & Wang, Z. Ecosystem effects of acidic deposition. In *Encyclopedia of Water: Science, Technology, and Society*, 1–12 (2019). https://doi.org/10.1002/9781119300762.wsts0043
36. Letcher, B. H. et al. Identifying mechanisms underlying individual body size increases in a changing, highly seasonal environment: The growing trout of West Brook. *J. Anim. Ecol.* **92**(1), 78–96. https://doi.org/10.1111/1365-2656.13833 (2023).
37. Smith, D. A. & Ridgway, M. S. Temperature selection in Brook Charr: lab experiments, field studies, and matching the Fry curve. *Hydrobiologia* **840**, 143–156. https://doi.org/10.1007/s10750-018-3869-4 (2019).
38. Jonsson, A. G. F. B. Effect of incubation temperature on growth performance in Atlantic salmon. *Mar. Ecol. Prog. Ser.* **454**, 75–82. https://doi.org/10.3354/meps09643 (2012).
39. Münz, H. Morphology and innervation of the lateral line system in *Sarotherodon niloticus* (L.) (Cichlidae, Teleostei). *Zoomorphologie* **93**(1), 73–86. https://doi.org/10.1007/BF02568676 (1979).
40. Kelly, J. T. et al. Evidence for episodic acidification effects on migrating Atlantic salmon *Salmo salar* smolts. *J. Fish Biol.* **87**(5), 1129–1146. https://doi.org/10.1111/jfb.12763 (2015).
41. Zdasiuk, B. J. et al. Evaluating acid-aluminum stress in streams of the Northeastern US at watershed, fish community and physiological scales. *Ecol. Ind.* **144**, 109480. https://doi.org/10.1016/j.ecolind.2022.109480 (2022).
42. Jesus, T. F. et al. Different ecophysiological responses of freshwater fish to warming and acidification. *Comp. Biochem. Physiol. A Mol. Integr. Physiol.* **216**, 34–41. https://doi.org/10.1016/j.cbpa.2017.11.007 (2018).
43. Kim, S. K. & Jung, W. K. Beneficial effect of teleost fish bone peptide as calcium supplements for bone mineralization. *Adv. Food Nutr. Res.* **65**, 287–295. https://doi.org/10.1016/B978-0-12-416003-3.00019-6 (2012).
44. Wiersinga-Post, J. E. C. & van Netten, S. M. Temperature dependency of cupular mechanics and hair cell frequency selectivity in the fish canal lateral line organ. *J. Comp. Physiol. A.* **186**, 949–956. https://doi.org/10.1007/s003590000147 (2000).
45. McHenry, M. J. & van Netten, S. M. The flexural stiffness of superficial neuromasts in the zebrafish (*Danio rerio*) lateral line. *J. Exp. Biol.* **210**(23), 4244–4253. https://doi.org/10.1242/jeb.009290 (2007).
46. Puschner, B. & Schacht, J. Energy metabolism in cochlear outer hair cells in vitro. *Hear. Res.* **114**(1–2), 102–106. https://doi.org/10.1016/S0378-5955(97)00163-9 (1997).
47. Taylor, R. R. & Forge, A. Hair cell regeneration in sensory epithelia from the inner ear of a urodele amphibian. *J. Comp. Neurol.* **484**(1), 105–120. https://doi.org/10.1002/cne.20450 (2005).
48. Baker, K. & Staecker, H. Low dose oxidative stress induces mitochondrial damage in hair cells. *Anat. Rec. Adv. Integr. Anat. Evol. Biol.* **295**(11), 1868–1876. https://doi.org/10.1002/ar.22594 (2012).
49. Carrillo, A. & McHenry, M. J. Zebrafish learn to forage in the dark. *J. Exp. Biol.* **219**(4), 582–589. https://doi.org/10.1242/jeb.128918 (2016).
50. Suli, A., Watson, G. M., Rubel, E. W. & Raible, D. W. Rheotaxis in larval zebrafish is mediated by lateral line mechanosensory hair cells. *PLoS ONE* **7**(2), e29727. https://doi.org/10.1371/journal.pone.0029727 (2012).
51. Nakae, M., Hasegawa, K. & Miyamoto, K. Domestication of captive-bred masu salmon *Oncorhynchus masou masou* (Salmonidae) leads to a significant decrease in numbers of lateral line organs. *Sci. Rep.* **12**(1), 16780. https://doi.org/10.1038/s41598-022-21195-3 (2023).
52. Williams, D. D. The first diets of postemergent brook trout (Salvelinus fontinalis) and Atlantic salmon (*Salmo salar*) alevins in a Quebec river. *Can. J. Fish. Aquat. Sci.* **38**(7), 765–771. https://doi.org/10.1139/f81-104 (1981).
53. Harper, M. P. & Peckarsky, B. L. Emergence cues of a mayfly in a high-altitude stream ecosystem: Potential response to climate change. *Ecol. Appl.* **16**(2), 612–621. https://doi.org/10.1890/1051-0761(2006)016[0612:ECOAMI]2.0.CO;2 (2006).
54. Rutherford, J. C., Blackett, S., Blackett, C., Saito, L. & Davies-Colley, R. J. Predicting the effects of shade on water temperature in small streams. *N. Z. J. Mar. Freshwat. Res.* **31**(5), 707–721. https://doi.org/10.1080/00288330.1997.9516801 (1997).
55. Forrester, G. E., Chace, J. G. & McCarthy, W. Diel and density-related changes in food consumption and prey selection by brook charr in a New Hampshire stream. *Environ. Biol. Fishes* **39**(3), 301–311 (1994).
56. Walsh, G., Morin, R. & Naiman, R. J. Daily rations, diel feeding activity and distribution of age-0 brook charr, *Salvelinus fontinalis*, in two subarctic streams. *Environ. Biol. Fishes* **21**(3), 195–205. https://doi.org/10.1007/BF00004863 (1988).
57. Johnson, J. H., Ross, R. M., Dropkin, D. S. & Redell, L. A. Ontogenetic and diel variation in stream habitat use by brook trout (*Salvelinus fontinalis*) in a headwater stream. *J. Freshw. Ecol.* **26**(1), 143–152. https://doi.org/10.1080/02705060.2011.553948 (2011).
58. Fischer, E. K., Soares, D., Archer, K. R., Ghalambor, C. K. & Hoke, K. L. Genetically and environmentally mediated divergence in lateral line morphology in the Trinidadian guppy (*Poecilia reticulata*). *J. Exp. Biol.* **216**(16), 3132–3142. https://doi.org/10.1242/jeb.081349 (2013).
59. Kelley, J. L., Grierson, P. F., Davies, P. M. & Collin, S. P. Water flows shape lateral line morphology in an arid zone freshwater fish. *Evol. Ecol. Res.* **18**(4), 411–428 (2017).

60. Cohen-Rengifo, M., Mazurais, D. & Bégout, M. L. Response to visual and mechano-acoustic predator cues is robust to ocean warming and acidification and is highly variable in European sea bass. *Front. Mar. Sci.* **10**, 1108968. https://doi.org/10.3389/fmars.2023.1108968 (2023).
61. Keenleyside, M. H. & Hoar, W. S. Effects of temperature on the responses of young salmon to water currents. *Behaviour* **7**, 77–87 (1954).
62. Brown, A. D., Sisneros, J. A., Jurasin, T., Nguyen, C. & Coffin, A. B. Differences in lateral line morphology between hatchery-and wild-origin steelhead. *PLoS ONE* **8**(3), e59162. https://doi.org/10.1371/journal.pone.0059162 (2013).
63. RStudio Team. RStudio: Integrated Development for R. RStudio, PBC (2020). http://www.rstudio.com/.
64. Muggeo, V. M. Interval estimation for the breakpoint in segmented regression: a smoothed score-based approach. *Aust. N. Z. J. Stat.* **59**, 311–322 (2017).
65. Potthoff, T. Clearing and staining techniques. In *Ontogeny and Systematics of Fishes* (eds Moser, H. G. et al.) 35–37 (Allen Press, 1984).

Acknowledgements

Work was funded by an NSF Graduate Research Fellowship (AEJ) and NSF INTERN supplemental funding (for support of AEJ, PI Brenton DeBoef, Dean of the Graduate School, URI), SICB Fellowship for Graduate Student Travel (AEJ), the George and Barbara Young Chair Endowment at URI (JFW), and the URI Graduate School (AEJ). Any use of trade, firm or product names is for descriptive purposes only and does not imply endorsement by the U.S. Government.

Author contributions

Aubree E. Jones—designed study, collected and analyzed data, wrote manuscript; Matthew O'Donnell—designed study, provided study material and facilities, edited manuscript; Amy Regish—designed study, provided study material and facilities, edited manuscript; Jacqueline F. Webb—designed study, supervised study, provided funding, edited and approved final manuscript.

Declarations

Competing interests

The authors declare no competing interests.

Additional information

Supplementary Information The online version contains supplementary material available at https://doi.org/10.1038/s41598-025-99784-1.

Correspondence and requests for materials should be addressed to A.E.J. or J.F.W.